Environmental and Ecological Statistics **9**, 89–110, 2002

A statistical evaluation of non-ergodic variogram estimators

FRANK C. CURRIERO,[1] MICHAEL E. HOHN,[2] ANDREW M. LIEBHOLD[3] and SUBHASH R. LELE[4]

[1]*Department of Biostatistics, The Johns Hopkins University, Baltimore, Maryland 21205, U.S.A. E-mail: fcurrier@jhsph.edu*
[2]*West Virginia Geological and Economic Survey, Morgantown, West Virginia 26505, U.S.A.*
[3]*USDA Forest Service, Northeastern Forest Experiment Station, Morgantown, West Virginia 26505, U.S.A.*
[4]*Department of Mathematical Sciences, University of Alberta Edmonton, AB T6G 2G1, Canada*

Received October 1999; Revised February 2001

Geostatistics is a set of statistical techniques that is increasingly used to characterize spatial dependence in spatially referenced ecological data. A common feature of geostatistics is predicting values at unsampled locations from nearby samples using the kriging algorithm. Modeling spatial dependence in sampled data is necessary before kriging and is usually accomplished with the variogram and its traditional estimator. Other types of estimators, known as non-ergodic estimators, have been used in ecological applications. Non-ergodic estimators were originally suggested as a method of choice when sampled data are preferentially located and exhibit a skewed frequency distribution. Preferentially located samples can occur, for example, when areas with high values are sampled more intensely than other areas. In earlier studies the visual appearance of variograms from traditional and non-ergodic estimators were compared. Here we evaluate the estimators' relative performance in prediction. We also show algebraically that a non-ergodic version of the variogram is equivalent to the traditional variogram estimator. Simulations, designed to investigate the effects of data skewness and preferential sampling on variogram estimation and kriging, showed the traditional variogram estimator outperforms the non-ergodic estimators under these conditions. We also analyzed data on carabid beetle abundance, which exhibited large-scale spatial variability (trend) and a skewed frequency distribution. Detrending data followed by robust estimation of the residual variogram is demonstrated to be a successful alternative to the non-ergodic approach.

Keywords: covariogram, correlogram, kriging, simulation, median-polish, robust variogram estimator

1. Introduction

A property exhibited by many data sets in ecology is that observations taken close together in space are more similar than observations taken further away. This is an example of

1352-8505 © 2002 Kluwer Academic Publishers

spatial dependence, generally defined to exist when data observed or measured depend to some degree on their relative spatial locations. Geostatistics is a set of statistical techniques used to analyze spatially dependent data. The use of geostatistics in ecology was introduced by Robertson (1987) and subsequently has gained in popularity (Legendre and Fortin, 1989; Rossi *et al.*, 1992; Hohn *et al.*, 1993; Liebhold *et al.*, 1995; Schlesinger *et al.,* 1996; Raty *et al.*, 1997; Robertson *et al.*, 1997; Koenig, 1999). Spatial dependence in geostatistics is commonly modeled with the variogram. In practice a variogram model, chosen from a pool of valid models (e.g., Journel and Huijbregts, 1978), is fit to a set of variogram estimates. This fitted model is then used, along with values from observed locations, in kriging, which provides predicted values at locations where values have not been sampled. Accuracy and precision of kriged predictions can depend on these fitted variogram models which in turn may be influenced greatly by the method used to first estimate the variogram.

The traditional variogram estimator (e.g., Cressie, 1991) has received most of the attention in practice. Isaaks and Srivastava (1988) and Srivastava and Parker (1989) propose other estimators of spatial dependence, called non-ergodic estimators. These estimators are claimed to perform well in situations where the observed data exhibit characteristics such as heteroscedasticity, skewness, or were preferentially sampled. Preferential samples can occur, for example, when areas with high values are sampled more intensely than other areas throughout the study domain. Rossi *et al.* (1992) used ecological data sets to visually compare the traditional variogram estimator to these non-ergodic estimators. They suggested that the non-ergodic approach may often be superior to the traditional variogram estimator for reproducing the true underlying spatial structure. This appears to have encouraged the use of non-ergodic estimators in several ecological applications (e.g., Rossi and Posa, 1990; Sharov *et al.*, 1997; Knudsen *et al.*, 1994). Non-ergodic estimators are also calculated by some popular computer packages offering geostatistical computations, for example, GSLIB (Deutsch and Journel, 1992), Variowin (Pannatier, 1996), and Splus Spatial Stats (Kaluzny *et al.*, 1996). This report investigates the traditional and non-ergodic estimation approaches to spatial dependence by extending the previous work based on visual comparisons to include performance in spatial prediction (kriging).

We first define the traditional and non-ergodic estimators and discuss their differences by explaining the calculations involved in computing each estimator. We show algebraically that in the omnidirectional case, a non-ergodic form of the variogram estimator is equivalent to the traditional estimator. We then propose a simulation study to compare the estimators' predictive performance, considering effects caused by data skewness and preferential sampling. The results and interpretations further clarify previous work with the non-ergodic estimators. The effect of large-scale spatial variability (trend) on variogram estimation is demonstrated using data collected on carabid beetles. Detrending the data and robust estimation of the residual variogram is demonstrated to be a successful alternative to the non-ergodic approach.

2. Methods

2.1 *Variogram estimators*

Variograms are used frequently in geostatistics to model spatial dependence, although covariograms and correlograms can also be used. In either case, the underlying model of spatial dependence in practice is rarely known. A common approach is to estimate the spatial dependence and then fit a parametric model to the estimated spatial pattern. Let

$$\{z(\boldsymbol{s}_1), \ldots, z(\boldsymbol{s}_n)\}$$

represent a set of spatial data where $\boldsymbol{s}_i$, $i = 1, \ldots, n$ denotes the observed spatial locations and $z(\cdot)$ the observed value at that location. The variogram, covariogram, and correlogram functions, denoted by $2\gamma(\cdot)$, $C(\cdot)$, and $\rho(\cdot)$ respectively, model spatial dependence between locations $\boldsymbol{s}_i$ and $\boldsymbol{s}_j$ as a function of the lag vector, $\boldsymbol{h} = \boldsymbol{s}_i - \boldsymbol{s}_j$. Spatial dependence is also assumed either isotropic, depending just on distance, denoted by the Euclidean metric $\|\boldsymbol{h}\|$, or anisotropic, depending on distance and direction.

The traditional estimator of the variogram is:

$$2\widehat{\gamma}(\boldsymbol{h}) = \frac{1}{|N(\boldsymbol{h})|}\sum_{N(\boldsymbol{h})}(z(\boldsymbol{s}_i) - z(\boldsymbol{s}_j))^2. \tag{1}$$

The set $N(\boldsymbol{h})$ contain the pairs of locations $(\boldsymbol{s}_i, \boldsymbol{s}_j)$ that are a distance $\|\boldsymbol{h}\|$ apart and $|N(\boldsymbol{h})|$ is the number of such pairs. Distances are usually grouped into distance classes by defining tolerance regions around $\|\boldsymbol{h}\|$. The semivariogram, $\gamma(\boldsymbol{h})$, is defined to be one half the variogram and can be estimated by just dividing (1) by a factor of 2. In the interest of brevity, many references in the field of ecology refer to $\gamma(\cdot)$ as the variogram instead of using the term semivariogram. The traditional estimator of the covariogram is:

$$\widehat{C}(\boldsymbol{h}) = \frac{1}{|N(\boldsymbol{h})|}\sum_{N(\boldsymbol{h})}(z(\boldsymbol{s}_i) - \bar{z})(z(\boldsymbol{s}_j) - \bar{z}), \tag{2}$$

where

$$\bar{z} = (1/n)\sum_{i=1}^{n} z(\boldsymbol{s}_i)$$

represents the mean of the sampled data. A traditional estimator of the correlogram can be obtained by

$$\widehat{\rho}(\boldsymbol{h}) = \frac{\widehat{C}(\boldsymbol{h})}{\widehat{C}(\boldsymbol{0})}, \tag{3}$$

where $\widehat{C}(\boldsymbol{0})$ represents an estimate of variance for the spatial process.

Under the assumption of second-order stationarity of the underlying spatial stochastic process, the variogram and covariogram models are related linearly through

$$2\gamma(\boldsymbol{h}) = 2C(\boldsymbol{0}) - 2C(\boldsymbol{h}). \tag{4}$$

The variogram and the estimator in (1), are used most often in practice. Reasons for preferring the variogram and its traditional estimator are based on issues of stationarity and unbiasedness (Cressie 1991, page 70–73).

In practice, variogram estimates can be calculated in different directions by first restricting the set of location-to-location pairs to only those that are within a given angle tolerance of the chosen directions. Visual inspection of such directional estimates are commonly used to determine isotropic or anisotropic behavior. For isotropic spatial dependence, an omnidirectional variogram is computed without regard to direction by combining all possible directions into one estimate.

Proponents of the deterministic (design-based) approach to geostatistics (e.g., Isaaks and Srivastava, 1988; Srivastava and Parker, 1989) question the preferred use of variogram estimation to covariogram estimation, which relies on model-based assumptions that may be of little practical importance. In their efforts to better characterize spatial dependence for a given data set in hand (as opposed to the traditional estimator which treats data as just one possible realization of the underlying model), they propose the following non-ergodic covariogram estimator,

$$\begin{aligned}\widehat{C}_{ne}(\boldsymbol{h}) &= \frac{1}{|N(\boldsymbol{h})|}\sum_{N(\boldsymbol{h})}(z(\boldsymbol{s}_i) - \bar{z}(\boldsymbol{h}_i))(z(\boldsymbol{s}_j) - \bar{z}(\boldsymbol{h}_j)) \\ &= \frac{1}{|N(\boldsymbol{h})|}\sum_{N(\boldsymbol{h})} z(\boldsymbol{s}_i)z(\boldsymbol{s}_j) - \bar{z}(\boldsymbol{h}_i)\bar{z}(\boldsymbol{h}_j),\end{aligned} \tag{5}$$

where the statistics $\bar{z}(\boldsymbol{h}_i)$ and $\bar{z}(\boldsymbol{h}_j)$ represent the mean of all observations appearing respectively as $z(\boldsymbol{s}_i)$ and $z(\boldsymbol{s}_j)$ in each set $N(\boldsymbol{h})$. This notation is referred to in Isaaks and Srivastava (1988) as the mean of the ''head'' and mean of the ''tail'' values, deriving its meaning from the head and tail of the vector separating two locations (Deutsch and Journel, 1992). The non-ergodic correlogram estimator is given as,

$$\widehat{\rho}_{ne}(\boldsymbol{h}) = \frac{\widehat{C}_{ne}(\boldsymbol{h})}{\widehat{\sigma}(\boldsymbol{h}_i)\widehat{\sigma}(\boldsymbol{h}_j)}, \tag{6}$$

where $\widehat{\sigma}(\boldsymbol{h}_i)$ and $\widehat{\sigma}(\boldsymbol{h}_j)$ represent similarly head and tail standard deviations. The term non-ergodic refers to a deterministic statistical model of only a single bounded realization (the data observed) without regard to expected values (moments) taken over all possible realizations (ergodicity).

There is a clear distinction between head and tail locations for one dimensional processes such as time series or spatial transects (e.g., Cox, 1983). When directional estimates are considered in the more general spatial setting (dimensions > 1), head and tail designations for a given pair of locations are defined by selecting, for example, the more north location as the head and the more south location as the tail for estimation in the north-south direction. Similar definitions apply when calculating estimates in the east-west direction, and so forth.

Defining head and tail values is meaningless for omnidirectional estimates. The common practice is to count each location twice, once as the head and once as the tail. This is equivalent to having the set $N(\boldsymbol{h})$ contain the location pairs $(\boldsymbol{s}_i, \boldsymbol{s}_j)$ as well as $(\boldsymbol{s}_j, \boldsymbol{s}_i)$ for all locations $\mathbf{s}_i, \mathbf{s}_j$ that are separated by a distance $\|\boldsymbol{h}\|$ (or are within the given tolerance region of $\|\boldsymbol{h}\|$). The resulting mean head values and mean tail values are thus equal, which simply corresponds to the mean of all the observations whose locations are separated by the given lag distance, referred to as the lag mean $\bar{z}(\boldsymbol{h})$. A similar argument can be used to combine head and tail standard deviations into one lag variance $\widehat{\sigma}^2(\boldsymbol{h})$ estimate. Therefore, omnidirectional non-ergodic covariogram and correlogram estimators can be written as

$$\widehat{C}_{ne}(\boldsymbol{h}) = \frac{1}{|N(\boldsymbol{h})|}\sum_{N(\boldsymbol{h})} z(\mathbf{s}_i)z(\mathbf{s}_j) - \bar{z}^2(\boldsymbol{h}), \tag{7}$$

and

$$\widehat{\rho}_{ne}(\boldsymbol{h}) = \frac{\widehat{C}_{ne}(\boldsymbol{h})}{\widehat{\sigma}^2(\boldsymbol{h})}.$$

Incidentally, the counting of each location twice does not effect any calculations in the traditional estimators (1) and (2).

2.2 *Traditional versus non-ergodic approach*

The difference between the traditional covariogram estimator (2) and the non-ergodic covariogram estimator (5) is the subtraction of a global mean versus the subtraction of ''local'' means. The term local is used in these non-ergodic estimators, not in the usual geographical sense, but to denote only those values contributing to that lag estimate, whether decomposed into head and tail attributes for directional estimates or one lag characteristic in the omnidirectional case. The non-ergodic correlogram estimator (6) incorporates a local variance in contrast to the constant (global) variance scaling factor used in the traditional correlogram estimator (3). It has been suggested that these alternative covariogram and correlogram estimators would provide for a more accurate characterization of spatial dependence by better accounting for peculiarities in spatial data through the changing local means and local variances (Isaaks and Srivastava, 1988; Srivastava and Parker, 1989; Rossi *et al*., 1992).

When omnidirectional estimates of spatial dependence are considered, the locations of data for any given distance class (denoted by $\boldsymbol{h}$) are spread over the entire spatial region under study. Clearly the data and number of location pairs contributing to each distance class differs across the lags. The local estimates of means and variances used in the non-ergodic estimators can be viewed as estimators of a global mean and variance based on smaller and different samples than that used in the traditional approach and thus likely to be poorer estimates of these parameters. Although this use of different data for each lag may be exactly what has been considered an advantage of the non-ergodic approach, it would appear to have a negative effect with stationary isotropic data, which by definition is characterized by a constant global mean and variance. The use of subsetted data would also appear to have a negative impact on estimation at the crucial shorter lags, where the number of available data pairs is often sparse.

In practice non-ergodic covariogram estimates are usually transformed, using relation (4), into variogram-like form by

$$2\widehat{C}(\mathbf{0}) - 2\widehat{C}_{ne}(\boldsymbol{h}), \tag{8}$$

where $\widehat{C}(\mathbf{0})$, an estimate of the total process variance, is required. Srivastava and Parker (1989) and Rossi *et al*. (1992) appear to use the sample variance $\widehat{\sigma}^2$ of the data

$z(\boldsymbol{s}_1), \ldots, z(\boldsymbol{s}_n)$ in (8) when graphically comparing the traditional and non-ergodic estimators. Barnes (1991), however, shows that taking $\widehat{C}(\boldsymbol{0}) = \widehat{\sigma}^2$ can either over- or underestimate $C(\boldsymbol{0})$ depending on the sampling configuration and possible trend contamination. One may wonder why the non-ergodic local variance estimate $\widehat{\sigma}(\boldsymbol{h}_i)\widehat{\sigma}(\boldsymbol{h}_j)$ is not used as $\widehat{C}(\boldsymbol{0})$ in (8) above, since the non-ergodic approach is based on these local statistics. It turns out, however (see appendix), that for the omnidirectional case such a procedure would just lead back to the traditional variogram estimator given in (1), that is

$$2\widehat{\gamma}(\boldsymbol{h}) = 2\widehat{\sigma}^2(\boldsymbol{h}) - 2\widehat{C}_{ne}(\boldsymbol{h}).$$

The variogram-like non-ergodic correlogram estimator is given by

$$2(1 - \widehat{\rho}_{ne}(\boldsymbol{h})), \tag{9}$$

which can be justified by combining (3) and (4). Semivariogram-like non-ergodic estimators can be obtained by dividing (8) and (9) by a factor of 2.

In practice, semivariogram models $\gamma(\boldsymbol{h})$ are usually fit to the estimated semivariogram, whether a traditional or non-ergodic approach has been adopted. Once a semivariogram $\gamma(\cdot)$ (or variogram) model has been specified it can be used in kriging. The kriging algorithm is designed to yield predictors that are linear, unbiased, and minimize mean-squared prediction error (e.g., Cressie, 1991, chapter 3). Let $\boldsymbol{s}_0$ represent a location where no data have been collected. The kriged value for $z(\boldsymbol{s}_0)$ is given by

$$\widehat{z}(\boldsymbol{s}_0) = \sum_{i=1}^{n} \lambda_i z(\boldsymbol{s}_i),$$

where weights, λ_i, $i = 1, \ldots, n$, are obtained by solving the following system of equations

$$\sum_{j=1}^{n} \lambda_j \gamma(\boldsymbol{s}_i - \boldsymbol{s}_j) - \gamma(\boldsymbol{s}_0 - \boldsymbol{s}_i) + m = 0, \qquad i = 1, \ldots, n \sum_{i=1}^{n} \lambda_i = 1. \tag{10}$$

The parameter m is a Lagrange multiplier used for constraining the predictor $\widehat{z}(\cdot)$ to be unbiased. The minimized mean-squared prediction error, often called the kriging variance, can also be calculated from (10).

As a result of (4), the above kriging equations can be equivalently written in terms of a covariogram or correlogram. Estimators of spatial dependence, both traditional and non-ergodic, however, are not related as simply as their model counterparts shown in (4). Thus differences in the kriging algorithm can result from choosing among the various estimators of spatial dependence.

2.3 *Simulation study*

We considered normal and lognormal spatial data, representing both symmetric and skewed frequency distributions, over a fixed two dimensional domain. The isotropic exponential semivariogram model,

$$\gamma(\boldsymbol{h}) = \begin{cases} 0 & \boldsymbol{h}=\boldsymbol{0} \\ c_0 + c_e\{1-\exp(-3\|\boldsymbol{h}\|/a_e)\} & \boldsymbol{h}\neq\boldsymbol{0} \end{cases} \tag{11}$$

was used as the true underlying model of spatial dependence with the sill parameter c_e and nugget parameter c_0 fixed at 25 and 5 respectively. The variogram range parameter a_e was set at 24, 48, and 96 representing relatively weak, medium, and strong levels of spatial dependence. Observations with these specifications were simulated using the LU decomposition of the covariance matrix (Davis, 1987) at locations on a 25×25 regular grid with 4 unit interval spacings, yielding an exhaustive set of 625 spatially dependent normal data for each variogram model specification. Lognormal data were simulated by exponentiating normal data generated with a sill of 1, a nugget of 0.2, and the same designated dependence levels.

The spatial data, once simulated, was considered fixed and then sampled using a regular grid and preferential type sampling designs. Regular grids are common sampling configurations used in ecology for collecting spatial data (Southwood, 1978; Greenwood, 1996). The use of such designs in practice does not knowingly produce spatially clustered and/or preferentially sampled observations. The regular grid samples in our simulations were obtained by extracting data from each exhaustive set using an 8 unit interval 13×13 regular grid. The preferential samples were obtained in a two stage process. An initial sample was first extracted from each exhaustive set using a 12 unit interval 9×9 regular grid. A second sample was then extracted (from the same exhaustive data set) in a neighborhood around only those 9×9 grid locations corresponding to the largest 12 values. The neighborhood was defined to be the closest eight neighbors on the original 4 unit interval grid around each selected location. Both samples were then combined. Because of the spatial dependence, such a procedure produced preferentially clustered samples of larger values and is similar to the adaptive sampling designs of Thompson (1990), which have been used in ecology (e.g., Thompson *et al.*, 1992; Smith *et al.*, 1995). Fig. 1 displays the regular grid configuration and an example preferential sampling configuration used in the simulations.

Let

$$\boldsymbol{S}_1 = \{\boldsymbol{s}_1, \ldots, \boldsymbol{s}_{n1}\},$$

represent the set of sampled spatial locations. For the regular grid designs $n1 = 169$ and the preferential sampling designs produced about the same sizes depending on how many locations in the initial sample were on the boundary of the domain (all eight neighbors could not be sampled for locations falling on the boundary). After specifying the set of sample locations $\boldsymbol{S}_1$ (either with the regular grid or preferential sampling procedure) an additional set of two hundred different locations were randomly selected from the remaining locations in each exhaustive set. These locations, denoted by the set

$$\boldsymbol{S}_2 = \{\boldsymbol{s}_{n1+1}, \ldots, \boldsymbol{s}_{n1+200}\},$$

represent locations for which kriged predictions will be sought. The simulated values at these locations, however, play no role in estimating and modeling the spatial dependence. They are taken to represent ''true'' values used for evaluating predictive performance. The locations in $\boldsymbol{S}_2$ do not remain fixed, rather were randomly selected each time data was simulated at $\boldsymbol{S}_1$.

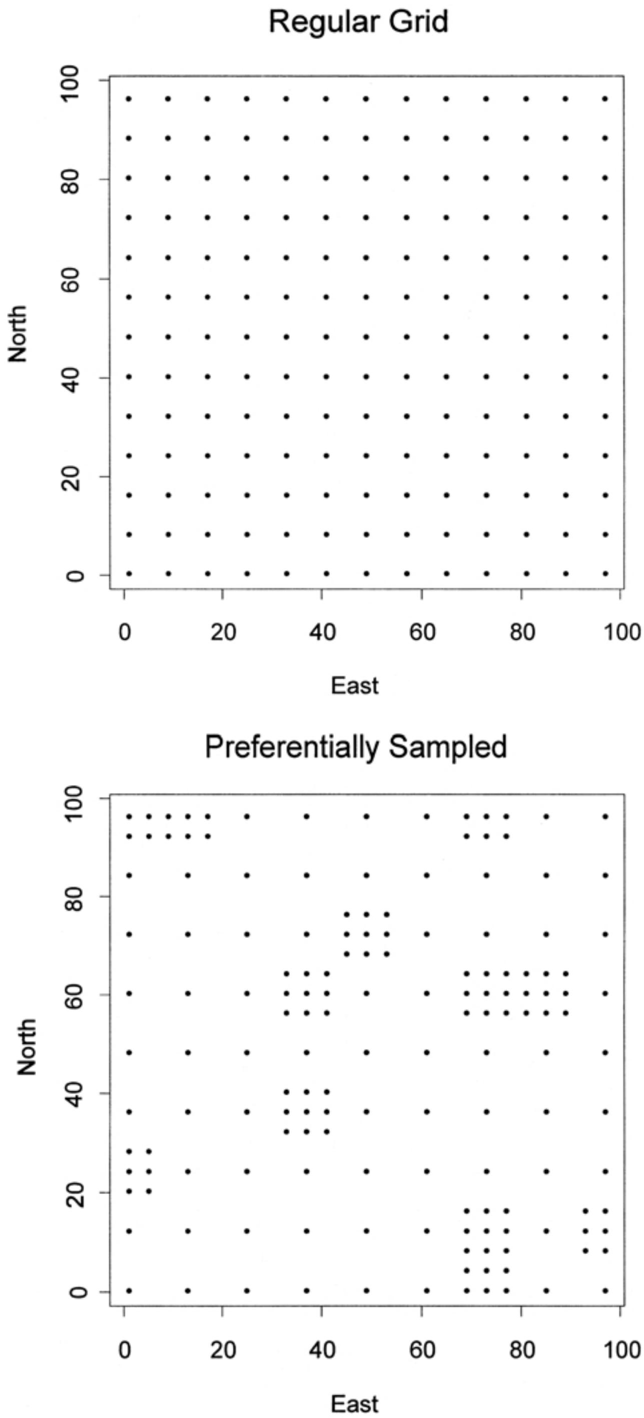

Figure 1. The regular grid and an example of a preferential sampling configuration used in the simulation study.

Let $\boldsymbol{Z}_1 = \{z(\boldsymbol{s}_1), \ldots, z(\boldsymbol{s}_{n1})\}$ and $\boldsymbol{Z}_2 = \{z(\boldsymbol{s}_{n1+1}), \ldots, z(\boldsymbol{s}_{n2})\}$ represent simulated data at the sampled $\boldsymbol{S}_1$ and unsampled $\boldsymbol{S}_2$ locations respectively. Isotropic exponential semivariogram models were fit using the weighted least squares (WLS) procedure of Cressie (1985) to omnidirectional semivariogram estimates based on $\boldsymbol{Z}_1$ using the traditional estimator (1) and the non-ergodic estimators (8) and (9). For lognormal data a semivariogram model was also fit to estimates based on the $\log_e$ transformed data using the traditional semivariogram estimator.

Performance of the traditional and non-ergodic variogram estimation procedures were evaluated based on the accuracy of resulting kriged predictions. Root mean squared prediction error (RMSPE) were calculated for each model fitted:

$$\text{RMSPE} = \left\{ \frac{1}{n2} \sum_{i=n1+1}^{n2} (z^*(\boldsymbol{s}_i) - z(\boldsymbol{s}_i))^2 \right\}^{1/2}, \tag{12}$$

where $z^*(\cdot)$ is the ordinary kriged prediction, using one of the models, and $z(\mathbf{s}_i)$ the ''true'' value. Predictions based on lognormal data were transformed back unbiasedly (e.g., Cressie, 1991, page 135) to the original scale. Efficiency ratios were generated by dividing the RMSPE based on the non-ergodic approach to those obtained using the traditional approach. Since smaller values of RMSPE are desired, ratios greater than 1.00 indicate favor towards the traditional semivariogram estimator. Ratios close to or less than 1.00 can be interpreted accordingly. For lognormal data, the efficiencies were calculated relative to the traditional approach based on the $\log_e$ transformed data.

The following algorithm summarizes the simulations.

Step 1 Select a data type (normal or lognormal), sampling design (regular grid or preferential), and spatial dependence level (weak, medium, or strong).

Step 2 Simulate an exhaustive data set with the above specifications. Sample this data set as specified yielding the sets $\boldsymbol{S}_1$, $\boldsymbol{S}_2$, $\boldsymbol{Z}_1$, and $\boldsymbol{Z}_2$.

Step 3 Fit isotropic exponential semivariogram models to the semivariogram estimates obtained from the traditional estimator (1) and the non-ergodic estimators (8) and (9). Generate kriged predictions at the locations in $\boldsymbol{S}_2$ using these fitted models.

Step 4 For each approach calculate the RMSPE statistic. Generate efficiency ratios by dividing these values for the non-ergodic approach by the corresponding value from the traditional approach.

Step 5 Repeat steps 2 through 4 500 times for each data type, sampling design, and variogram dependence level combination specified in Step 1.

All data simulation, semivariogram estimation, and kriging were performed using Splus (MathSoft Inc., 1995) and Splus Spatial Stats (Kaluzny *et al*., 1996). Semivariogram models were fit using SAS procedure NLIN (SAS Institute, 1990). Note, the omnidirectional non-ergodic covariogram and correlogram estimators were calculated by setting the angle tolerances (*tol.azimuth* argument) to a value greater than 90 in the Splus Spatial Stats covariogram and correlogram functions, which adjusts for an apparent bug in this release (Silvia C. Vega, personal communication).

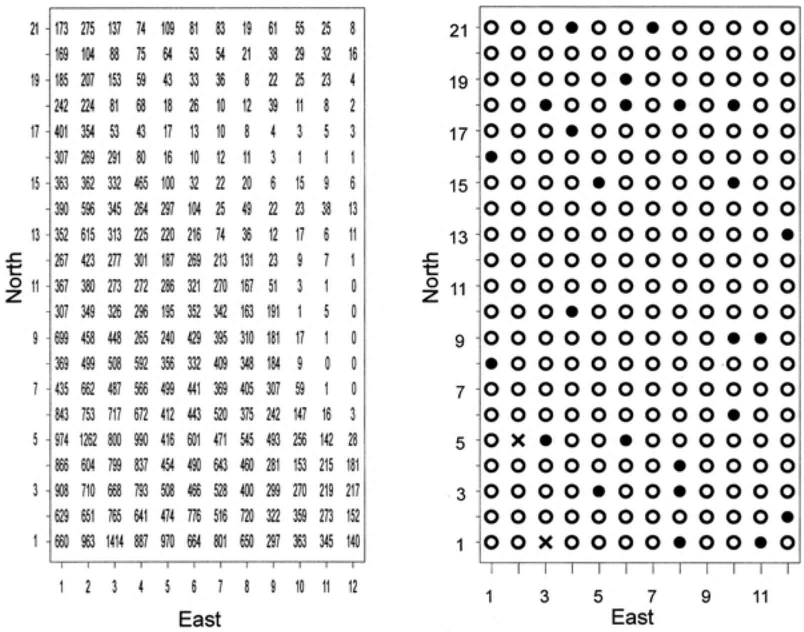

Figure 2. Data posting (left) of Hengeveld's (1979) carabid beetle, *Pterostichus coerulescens*, counts. Each unit interval spacing in both the directions represent 40 m. Locations (right) representing the sampled 225 observations ○ and the 25 observations • set aside to evaluate prediction. Locations of the two outliers excluded from the analyzes are labeled with an ×.

2.4 *Analyses of Hengeveld's beetle data*

Hengeveld (1979, Table 2) provides pitfall trap count data on the carabid beetle, *Pterostichus coerulescens*. We compare predictive performance of methods used to characterize spatial dependence in these beetle counts. We choose this data because it was one of the examples considered in Rossi *et al.* (1992) where traditional and non-ergodic estimates of spatial variability were examined visually. We extend this examination to include spatial prediction. Analyses presented below are for demonstration purposes only. The methods employed do not represent the only possible approaches nor do they represent necessarily a best approach.

The spatial data posted in Fig. 2 (left) consists of 252 observations (beetle trap counts) referenced by their corresponding locations, labeled here arbitrarily as representing an east and north coordinate. Two observations (counts of 1262 and 1414) in the southwest corner were beyond 3 (and almost 4) standard deviations of the mean and considered as possible outliers. So as not to have these anomalous values possibly effect our variogram comparisons they were excluded from subsequent analyzes. In a manner similar to the simulation study (with data sets $\boldsymbol{S}_1$ and $\boldsymbol{S}_2$), 25 observations were drawn randomly and set aside, Fig. 2 (right). Geostatistics was performed on the remaining 225 observations and used to generate kriged predictions at locations corresponding to the 25 observations set aside. Root mean squared error in prediction RMSPE statistics, as defined in (12), were

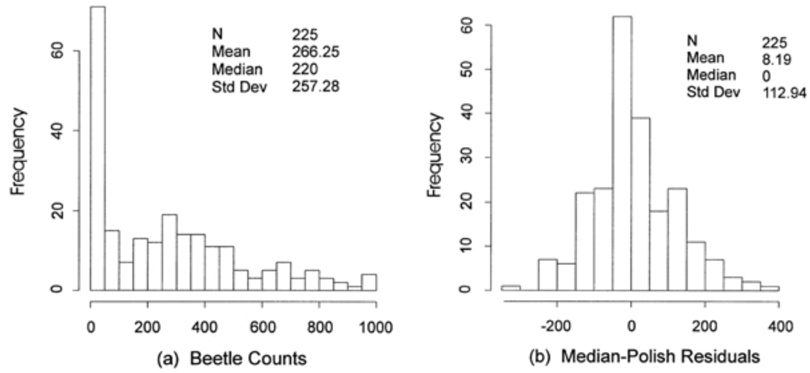

Figure 3. Frequency histograms for (a) the 225 sampled beetle counts and (b) the corresponding median-polish residuals.

used to evaluate prediction performance resulting from the use of different estimators of spatial dependence.

Because the 225 samples were drawn randomly from the 12×21 regular grid, there is no bias due to preferential sampling. There are two features of this data, however, that are interesting in regard to non-ergodic estimators of spatial dependence. First, the observations exhibit a skewed frequency distribution (Fig. 3a). Second, a linear interpolated surface shown in Fig. 4a appears to indicate a trend (i.e., a nonconstant mean) in the northeast to southwest direction. These two characteristics are known to adversely effect the traditional variogram estimator (e.g., Starks and Fang, 1982; Rossi *et al.*, 1992).

Our analyses of this data included kriged predictions based on semivariogram models fit to non-ergodic covariogram and correlogram estimates. Comparisons were made to an approach based first on detrending the data using median-polish (Cressie, 1991, Section 3.5) and estimating spatial dependence of the residuals. As a precaution, the robust semivariogram estimator of Cressie and Hawkins (1980),

$$\tilde{\gamma}(\boldsymbol{h}) = \left\{ \frac{1}{2|N(\boldsymbol{h})|} \sum_{N(\boldsymbol{h})} |Z(\boldsymbol{s}_i) - Z(\boldsymbol{s}_j)|^{1/2} \right\}^4 \Big/ (0.457 + 0.494/|N(\boldsymbol{h})|), \tag{13}$$

was used for the residuals, where the sets $N(\boldsymbol{h})$ are subject to the same distance grouping as for the other spatial dependence estimators defined previously. The estimator in (13) down-weights the influence of possible outliers. We did not consider this estimator in the simulation study because the problem of outliers did not arise. This robust semivariogram estimator is another alternative approach to dealing with certain peculiarities in spatial data.

3. Results

Each simulation experiment consisted of 500 analyses arising from combinations of data distribution type (normal and lognormal), sampling design (regular grid or preferential), and spatial dependence level (weak, medium, and strong). Of primary interest is the performance of the non-ergodic estimators compared to the traditional estimator, as

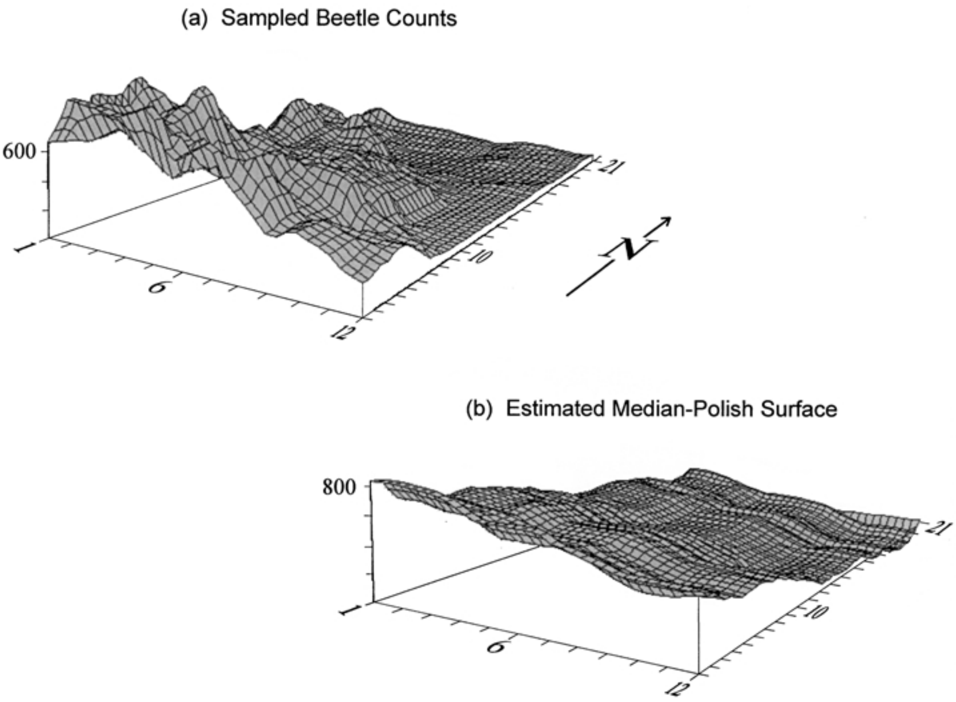

Figure 4. Orthographic perspective displays for (a) the sampled beetle counts and (b) the estimated median-polish trend surface.

measured by the RMSPE efficiency ratios. Tables 1 and 2 show, for each experiment, the percentage of these ratios that were greater than one, that is, percentage of times out of the 500 iterations that the analysis based on the traditional variogram estimator outperformed the analysis based on the non-ergodic estimators. Since this may be regarded as averaging over repeated realizations, an issue advocates of the non-ergodic approach may criticize, we have included Figs 5 and 6 which show distributional summaries of these ratios from which intepretations are made without regard to averaging or other summary measures over the simulations.

3.1 *Normal data with regular grid sampling*

Combining regular grid sampling with data generated from a spatially isotropic normal distribution represents the most ''well behaved'' scenario we considered; no advantage of the non-ergodic over the traditional estimator is expected. Table 1 indicates little difference in performance between the traditional and non-ergodic estimators: most percentages are around 50%. Some exceptions favoring the non-ergodic approach, however, were observed. For example, when predicting at unsampled locations, semivariogram models fit to estimates based on the non-ergodic correlogram estimator outperformed the models based on the traditional semivariogram estimator notably more often for the medium and strong levels of spatial dependence. However, as shown in Fig. 5

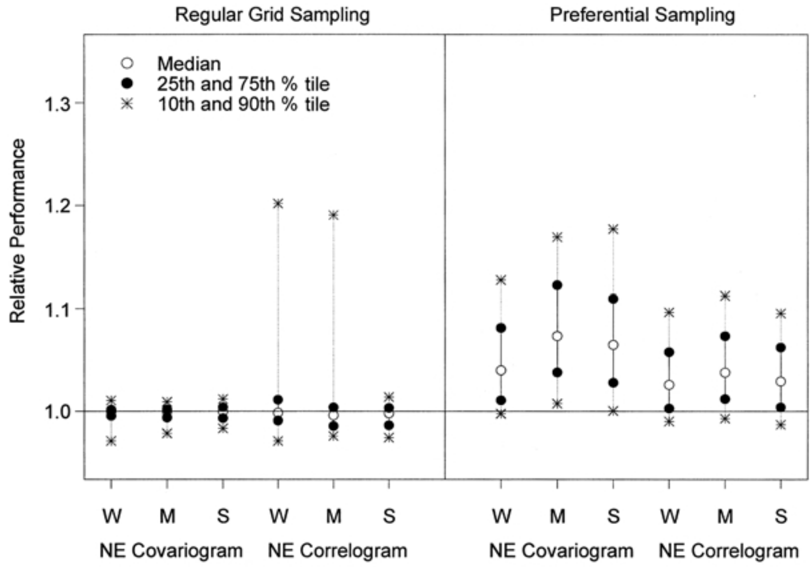

Figure 5. Distributional summaries for the simulated RMSPE efficiency ratios. Regular grid and preferential sampling were used with isotropic normal spatial data with weak (W), medium (M), and strong (S) levels of spatial dependence.

(left), there was a tendency for the non-ergodic correlogram estimator to lead to predictions that were about 20% less accurate than those based on the traditional semivariogram estimator.

3.2 *Normal data with preferential sampling*

In this spatial design scenario we considered data generated from a spatially isotropic normal distribution as above. However, samples were collected preferentially. Results shown in Table 1 clearly favor the traditional approach. At least 80% of the time the traditional semivariogram estimator produced more accurate predictions than either non-ergodic estimators. For half of the experiments these percentages were above 90%. The distributional summaries shown in Fig. 5 (right) provides information on the extent to which the traditional semivariogram estimator outperformed the non-ergodic estimators with respect to RMSPE.

3.3 *Lognormal data with regular grid sampling*

Data analyzed in this design were generated to be spatially isotropic and lognormal, representing a skewed frequency distribution, and sampled from a regular grid. Recall that for lognormal data we also considered analyses using the traditional semivariogram estimator based on the $\log_e$ transformed data as well as on the untransformed data. Results in Table 2 are expressed relative to the transformed data analysis. More than 68% of the time this traditional approach produced smaller RMSPE statistics than those obtained from

Table 1. Simulation results based on normal data with regular grid and preferential sampling. The values listed are the percentage of times the traditional variogram estimator outperformed the non-ergodic covariogram (NE Cov) and the non-ergodic correlogram (NE Corr) estimators.

		RMSEP	
Sampling Design	*Spatial Dependence*	*NE Cov*	*NE Corr*
	Weak	44.5%	44.9%
Regular Grid	Medium	41.5%	37.3%
	Strong	45.9%	38.7%
	Weak	88.0%	80.8%
Preferential	Medium	93.8%	86.0%
	Strong	90.0%	81.0%

Table 2. Simulation results based on lognormal data with regular grid and preferential sampling. The values listed are the percentage of times the traditional variogram estimator based on the $\log_e$ transformed data outperformed analyses based on the untransformed data using the traditional variogram (Tr Var), the non-ergodic covariogram (NE Cov), and the non-ergodic correlogram (NE Corr) estimators.

		RMSEP		
Sampling Design	*Spatial Dependence*	*Tr Var*	*NE Cov*	*NE Corr*
	Weak	77.4%	75.4%	73.1%
Regular Grid	Medium	79.4%	73.5%	72.9%
	Strong	76.2%	68.9%	68.3%
	Weak	98.2%	78.6%	78.8%
Preferential	Medium	99.2%	81.4%	86.2%
	Strong	98.6%	83.4%	85.8%

either non-ergodic estimators based on untransformed data. With respect to just the traditional semivariogram estimator, transforming the data was more successful (at least 76% of the time) than not transforming. Distributional summaries for the RMSPE efficiencies are provided in Fig. 6 (left).

3.4 *Lognormal data with preferential sampling*

In this design we considered preferentially sampled data with the skewed lognormal distributed. This spatial design represents the most ''misbehaved'' scenario we considered and is similar to the design used in Srivastava and Parker (1989). At least 78% of the time more accurate predictions were obtained with the traditional semivariogram estimator on the $\log_e$ transformed data than either of the non-ergodic estimators on untransformed data (Table 2). Preferential sampling also caused more of an effect with respect to the

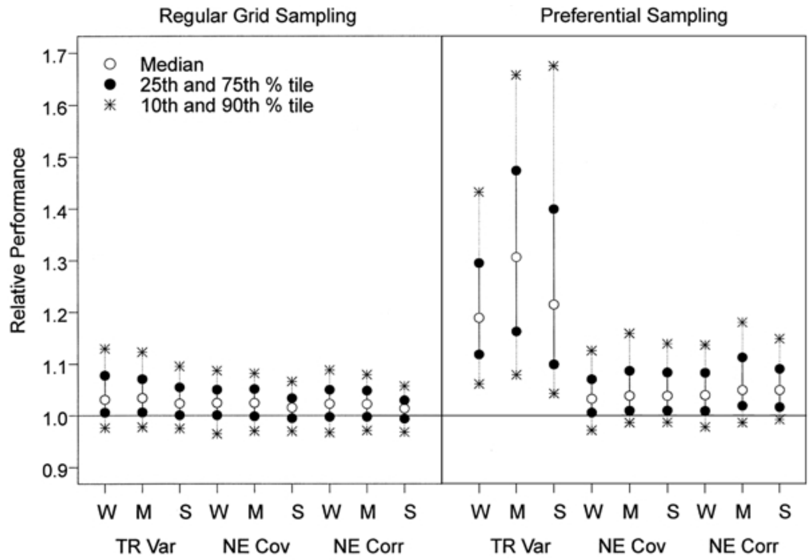

Figure 6. Distributional summaries for the simulated RMSPE efficiency ratios. Regular grid and preferential sampling were used with isotropic lognormal spatial data with weak (W), medium (M), and strong (S) levels of spatial dependence. Results for the traditional variogram (TR Var), non-ergodic covariogram (NE Cov), and non-ergodic correlogram (Ne Corr) were based on the untransformed lognormal data and taken relative to the traditional variogram on the $\log_e$ transformed data.

traditional semivariogram estimator on transformed and untransformed data than did the corresponding regular grid sampling results.

The non-ergodic approach produced results closer to those obtained from the transformed analyzes than did the traditional semivariogram estimator on the same untransformed data, Fig. 6 (right). Lag means and lag variances used in the non-ergodic estimators appear to have had a positive effect on this type of preferentially sampled lognormal data. Examples of the traditional semivariogram estimator based on the untransformed data were very erratic. Srivastava and Parker (1989) provide illustrations of this for a similar scenario. Fitting semivariogram models to these erratic estimates (not tabulated) and proceeding with kriging is highly questionable.

3.5 *Analyses of Hengeveld's beetle data*

Directional semivariogram estimates using the traditional estimator given in (1) are shown in Fig. 7a. Most of these estimates appear to increase without bound (linear in shape) at a rate which is direction dependent (anisotropic). The semivariogram estimates in the 135° direction, perpendicular to the apparent trend, however, indicate lack of spatial dependence. Figs 7b and 7c display directional non-ergodic covariogram and correlogram estimates using the estimators given in (8) and (9). Both non-ergodic estimators reveal an

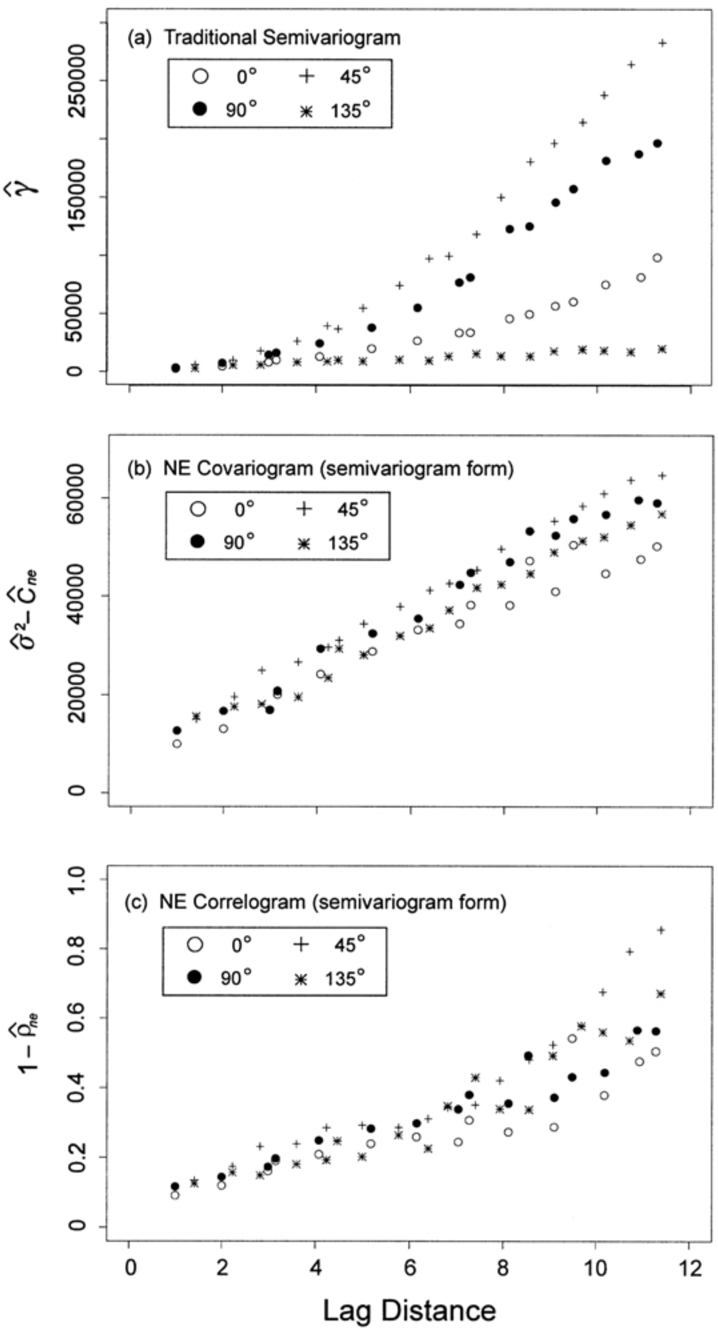

Figure 7. Directional semivariogram estimates based on the 225 sampled beetle counts using (a) the traditional semivariogram estimator, (b) the non-ergodic covariogram estimator, and (c) the non-ergodic correlogram estimator. The non-ergodic estimates are displayed in semivariogram-like form. Angular directions were measured clockwise from the 0° north-south direction using angle tolerances of 22.5°.

almost linear shaped model with isotropic spatial dependence, apparently masking the effect due to the trend. Power semivariogram models (e.g., Cressie, 1991, page 62), which include the linear model as a special case, were fit to the non-ergodic estimated isotropic patterns using the WLS procedure of Cressie (1985). Results are shown in Figs 8b and 8c.

More difficulty was encountered in modeling the behavior exhibited by the traditional semivariogram estimator shown in Fig. 7a. One approach could have been an attempt to model the anisotropic behavior. We adopted an alternative approach, which seemed reasonable for this example, based first on detrending the data and investigating spatial patterns of the residuals. We employed the median-polish kriging approach of Cressie (1991, Section 3.5). Fig. 4b shows the results of the fitted median-polish trend surface. The residuals, defined to be the actual beetle counts minus the median-polish estimate at that location, were used for variography.

Figure 3b displays the frequency distribution of the median-polish residuals, which is no longer skewed and appears approximately Gaussian shaped about a mean of zero. A linear interpolated plot of the residuals, similar to the ones displayed in Fig. 4, revealed no evidence of a trend. Based on directional semivariogram estimates, spatial dependence in the residuals was assumed isotropic. Fig. 8a displays this estimated isotropic pattern with a WLS fitted spherical semivariogram model. The distribution of the median-polish residuals shown in Fig. 3b, although seemingly ''well-behaved,'' does appear to contain possible outliers, both positive and negative. Estimates in Fig. 8a were thus based on the robust semivariogram estimator in (13). Although non-ergodic estimators could have also been used on residuals, this was made uncecessary by the median polish.

Ordinary kriging was performed using the semivariogram models shown in Fig. 8. Results (Table 3) show that RMSPE's were lowest for the approach based on median polish kriging. The relative gain over the non-ergodic approach was approximately 7% with respect to the non-ergodic covariogram and approximately 6% with respect to the non-ergodic correlogram.

Differences in prediction errors observed for the beetle data are not large and may not adequately justify the more complicated approach of decomposing the beetle counts into trend plus spatial dependence. Many applications in ecology focus on describing spatial dependence (e.g., Rossie *et al.*, 1992), rather than using the modeled spatial dependence as an intermediate step towards prediction. In these situations the variography results, such as those shown in Figs 7 and 8 for the beetle data, are of most interest. Practitioners may find it easier, however, to interpret the semivariogram in Fig. 8a in conjunction with the median-polish surface in Fig. 4b, than to understand the non-ergodic covariogram or correlogram.

Table 3. Root mean squared error in prediction results from the analyses of Hengeveld's carabid beetle data.

Modeling Approach	*RMSEP*
Median-Polish Robust Variogram	59.27
Non-Ergodic Covariogram	63.94
Non-Ergodic Correlogram	62.76

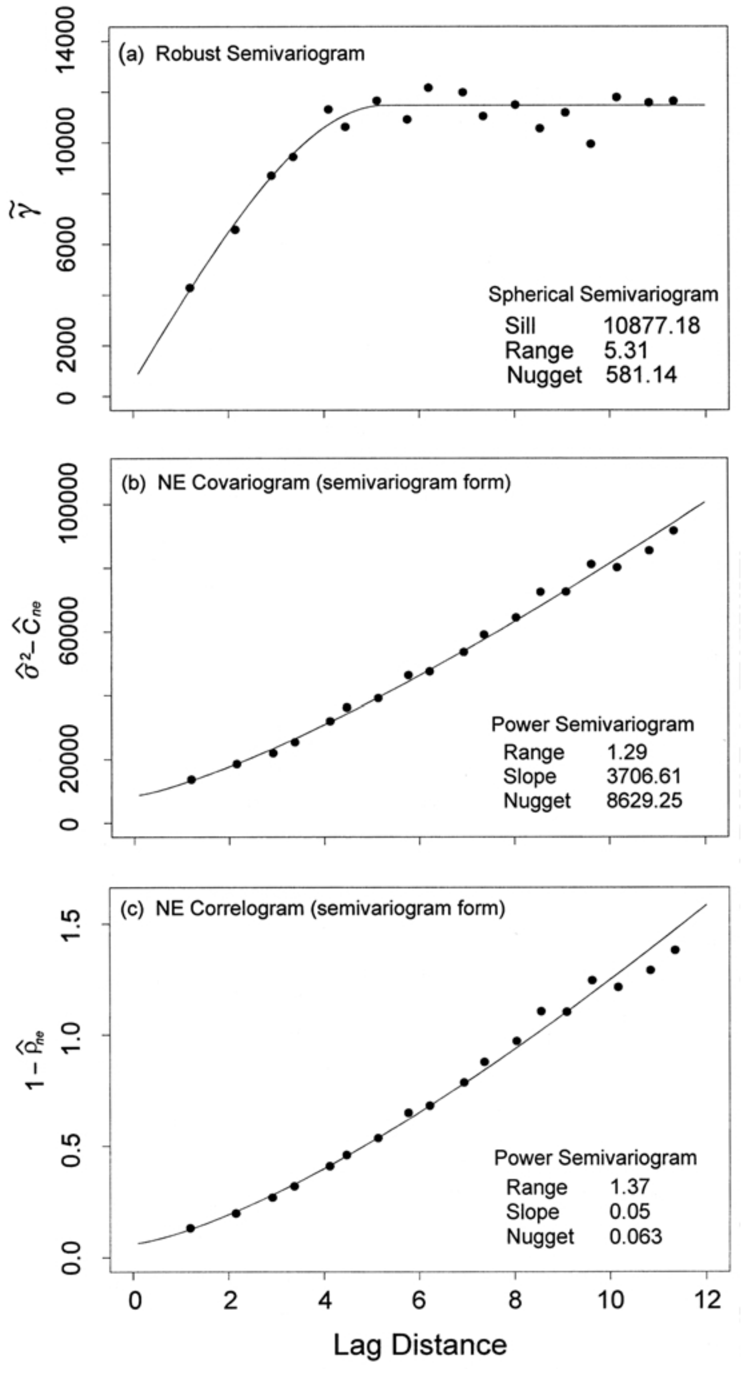

Figure 8. Weighted least squares fitted semivariogram models. (a) Spherical model fit to the isotropic pattern indicated by the robust semivariogram estimator based on the median-polish residuals. Power models fit to the isotropic patterns indicated by (b) the non-ergodic covariogram estimator and (c) the non-ergodic correlogram estimator.

4. Discussion

Variogram estimation is a crucial step in the geostatistical process. Non-ergodic estimators have been suggested as a preferred approach for analyzing data that depart from conditions in which the traditional variogram estimator is expected to perform well, such as skewed or preferentially sampled data. This conjecture appears to be based on earlier studies which visually compared traditional and non-ergodic estimators.

Designed to study the estimator's predictive performance, results from our simulations showed that traditional variogram estimation led to an increase in prediction accuracy more often than non-ergodic variogram estimation. Furthermore, the potential gains in predictive performance with the traditional approach (Figs 5 and 6) tended to be substantially greater than that potentially lost for non-ergodic approach. With respect to lognormal data, these results were based on traditional variogram estimation and kriging on the $\log_e$ transformed scale, which just transforms the data to normality. Basing the non-ergodic estimators on this transformed scale, besides eliminating the skewness property of the data, actually corresponds to the normal based experiments where the traditional approach was demonstrated to be superior, especially with preferential sampling.

All the simulations we considered were based on stationary isotropic data and the results, based on comments made in Section 2.2, may arguably have been predicted. We agree in regards to the Normal regular grid sampling scenario, however, it was unclear how the non-ergodic approach would perform with the additional effects of preferential sampling and heteroscedasticity, which is precisely the situation it has been proposed as the preferred method.

Lack of theoretical foundation with the non-ergodic estimators and our simulation results support variogram estimation via the traditional approach. Data in reality, however, will only at best approximate distributions such as normality or lognormality. To help characterize spatial dependence in these situations, practitioners can study the behavior of variograms using different estimators, a point suggested in Rossi *et al.* (1992) with respect to the traditional and non-ergodic estimators. Differences or similarities in such behavior along with other exploratory data analysis techniques can provide valuable information for estimating and modeling spatial dependence.

We conclude that the non-ergodic covariogram and correlogram possess no clear advantage over the traditional variogram for studying spatial dependence or making spatial predictions. In fact, as we have shown in the omnidirectional case, the non-ergodic form of the variogram estimator is equivalent to the traditional variogram estimator when the non-ergodic local estimates of mean and variance are used consistently throughout. Rather than depend upon these non-ergodic statistics, the practitioner is better served by applying appropriate transformations to skewed data, accounting for spatial trends, and recognizing the presence of preferential sampling or being aware of the effects of preferential sampling on measures of spatial dependence. Non-ergodic covariograms or correlograms cannot replace thorough data analysis before variography and prediction.

Acknowledgments

Frank C. Curriero's work was supported by a grant from the USDA CSREES Competitive Grants Program (95-37302-1905) which also partially supported the work from Michael E.

Hohn and Andrew M. Liebhold. Subhash Lele's contribution was supported by a grant from the Department of Energy (DE-FC07-94, Professor Daniel Goodman PI) and the US Environmental Protection Agency (STAR Grant R824995, Jonathan Patz PI). The authors express their appreciation to the anonymous referee's for their many helpful suggestions.

Appendix

Below we show algebraically that

$$\widehat{\gamma}(\boldsymbol{h}) = \widehat{\sigma}^2(\boldsymbol{h}) - \widehat{C}_{ne}(\boldsymbol{h}),$$

where $\widehat{\gamma}(\boldsymbol{h})$ is the traditional semivariogram estimator obtained from (1) and $\widehat{C}_{ne}(\boldsymbol{h})$ is the omnidirectional non-ergodic covariogram estimator defined in (7). Let the set $N(\boldsymbol{h})$ contain the pairs of locations $(\boldsymbol{s}_i, \boldsymbol{s}_j)$ as well as $(\boldsymbol{s}_j, \boldsymbol{s}_i)$ that are a distance $\|\boldsymbol{h}\|$ apart. An estimate of lag variance can then be given by

$$\widehat{\sigma}^2(\boldsymbol{h}) = \frac{1}{|N(\boldsymbol{h})|}\sum_{N(\boldsymbol{h})}(z(\boldsymbol{s}_i) - \bar{z}(\boldsymbol{h}))^2 = \frac{1}{|N(\boldsymbol{h})|}\sum_{N(\boldsymbol{h})}z(\boldsymbol{s}_i)^2 - \bar{z}^2(\boldsymbol{h}),$$

where $\bar{z}(\boldsymbol{h})$ is an estimate of lag mean,

$$\bar{z}(\boldsymbol{h}) = \frac{1}{|N(\boldsymbol{h})|}\sum_{N(\boldsymbol{h})}z(\boldsymbol{s}_i).$$

Then,

$$\begin{aligned}
\widehat{\gamma}(\boldsymbol{h}) &= \frac{1}{2|N(\boldsymbol{h})|}\sum_{N(\boldsymbol{h})}(z(\boldsymbol{s}_i) - z(\boldsymbol{s}_j))^2 \\
&= \frac{1}{2|N(\boldsymbol{h})|}\left(\sum_{N(\boldsymbol{h})}z(\boldsymbol{s}_i)^2 + \sum_{N(\boldsymbol{h})}z(\boldsymbol{s}_j)^2 - 2\sum_{N(\boldsymbol{h})}z(\boldsymbol{s}_i)z(\boldsymbol{s}_j)\right) \\
&= \frac{1}{|N(\boldsymbol{h})|}\sum_{N(\boldsymbol{h})}z(\boldsymbol{s}_i)^2 - \frac{1}{|N(\boldsymbol{h})|}\sum_{N(\boldsymbol{h})}z(\boldsymbol{s}_i)z(\boldsymbol{s}_j) \\
&= \frac{1}{|N(\boldsymbol{h})|}\sum_{N(\boldsymbol{h})}z(\boldsymbol{s}_i)^2 - \bar{z}^2(\boldsymbol{h}) - \left(\frac{1}{|N(\boldsymbol{h})|}\sum_{N(\boldsymbol{h})}z(\boldsymbol{s}_i)z(\boldsymbol{s}_j) - \bar{z}^2(\boldsymbol{h})\right) \\
&= \widehat{\sigma}^2(\boldsymbol{h}) - \widehat{C}_{ne}(\boldsymbol{h}).
\end{aligned}$$

References

Barnes, R.J. (1991) The variogram sill and sample variance. *Mathematical Geology*, **23**, 673–8.

Cressie, N. (1985) Fitting variogram models by weighted least squares. *Mathematical Geology*, **17**, 563–86.

Cressie, N. (1991) *Statistics for Spatial Data*, John Wiley and Sons, New York.

Cressie, N. and Hawkins, D.M. (1980) Robust estimation of the variogram: I. *Mathematical Geology*, **12**, 115–26.

Cox, N.J. (1983) On the estimation of spatial autocorrelation in geomorphology. *Earth Surface Processes and Landforms*, **8**, 89–93.

Davis, M. (1987) Production of conditional simulations via the LU decomposition of the covariance matrix. *Mathematical Geology*, **19**, 91–8.

Deutsch, C.V. and Journel, A.G. (1992) *GSLIB: Geostatistical Software Library*, Oxford University Press, New York.

Greenwood, J.J.D. (1996) Basic techniques, in *Ecological Census Techniques*, W.J. Sutherland (ed.), Cambridge University Press, New York, pp. 11–109.

Hohn, M.E., Liebhold, A.M., and Gribko, L.S. (1993) Geostatistical model for forecasting spatial dynamics of defoliation caused by the gypsy moth (Lepidoptera: Lymantriidae). *Environmental Entomology*, **22**, 1066–75.

Hengeveld, R. (1979) The analysis of spatial patterns of some ground beetles (col. Carrbidae), in *Spatial and Temporal Analysis in Ecology*, R.M. Cormack and J.K. Ord (eds), International Co-operative Publishing House.

Isaaks, E.H. and Srivastava, R.M. (1988) Spatial continuity measures for probabilistic and deterministic geostatistics. *Mathematical Geology*, **20**, 313–41.

Isaaks, E.H. and Srivastava, R.M. (1989) *An Introduction to Applied Geostatistics*, Oxford University Press, New York.

Journel, A.G. and Huijbregts, C.J. (1978) *Mining Geostatistics*, Academic Press, New York.

Kaluzny, S.P., Vega, S.C., Cardoso, T.P., and Shelly, A.A. (1996) *S + SPATIALSTATS, User's Manual*, MathSoft, Seattle.

Knudsen, G.R., Schotzka, D.J., and Krag, C.R. (1994) Fungal Entomopathogen effect on numbers and spatial patterns of the Russian Wheat Aphid (Homoptera: Aphididae) on preferred and nonpreferred host plants. *Environmental Entomology*, **23**, 1558–67.

Koenig, W.D. (1999) Spatial autocorrelation of ecological phenomena. *Trends in Ecology and Evolution*, **14**, 22–6.

Liebhold, A.M., Elkington, J.S., Zhou, G., Hohn, M.E., Rossi, R.E., Boettner, G.H., Boettner, C.W., Burnham, C., and McManus, M.L. (1995) Regional correlation of gypsy moth (Lepidoptera: Lymantriidae) defoliation with counts of egg masses, pupae, and male moths. *Environmental Entomology*, **24**, 193–203.

Legendre, P. and Fortin, M.J. (1989) Spatial pattern and ecological analysis. *Vegetatio*, **80**, 107–38.

MathSoft Inc. (1995) *S-PLUS User's Manual*, Version 3.3 for Windows, MathSoft, Seattle.

Pannatier, Y. (1996) *Variowin: Software for Spatial Data Analysis in 2D*, Springer-Verlag, New York.

Raty, L., Ciornei, C., and Mihalciuc, V. (1997) Spatio-temporal geostatistical analysis of *Ips typographus* monitoring catches in two Romanian forest districts. In *Proceedings: Integrating Cultural Tactics into the Management of Bark Beetle and Reforestation Pests*, J.C. Gregoire, A.M. Liebhold, F.M. Stephen, K.R. Day, and S.M. Salmon (eds), USDA Forest Service General Technical Report (in press).

Robertson, G.P. (1987) Geostatistics in ecology: interpolating with known variance. *Ecology*, **68**, 744–8.

Robertson, G.P., Klingensmith, K.M., Klug, M.J., Paul, E.A., Crum, J.R., and Ellis, B.G. (1997) Soil resources, microbial activity, and primary production across an agricultural ecosystem. *Ecological Applications*, **7**, 158–70.

Rossi, M. and Posa, D. (1990) 3-D mapping of dissolved oxygen in Mar Piccolo: A case study. *Enviornmental Geological Water Science*, **16**, 209–19.

Rossi, R.E., Mulla, D.J., and Journal, A.J. (1992) Geostatistical tools for modeling and interpreting ecological spatial dependence. *Ecological Monographs*, **62**, 277–314.

SAS Institute Inc. (1990) *SAS/STAT User's Guide, Version 6*. SAS Institute, North Carolina.

Schlesinger, W.H., Raikes, J.A., Hartley, A.E., and Cross, A.F. (1996) On the spatial pattern of soil nutrients in desert ecosystems. *Ecology*, **77**, 364–74.

Sharov, A.A., Liebhold, A.M., and Roberts, E.A. (1997) Methods for monitoring the spread of gypsy moth (Lepidoptera: Lymantriidae) populations in North America. *Journal of Economic Entomology* (in press).

Smith, D.R., Conroy, M.J., and Brakhage, D.H. (1995) Efficiency of adaptive cluster sampling for estimating density of wintering waterfowl. *Biometrics*, **51**, 777–88.

Southwood, T.R.E. (1978) *Ecological Methods*, Chapman and Hall, London.

Srivastava, R.M. and Parker, H.M. (1989) Robust measures of spatial continuity, in *Geostatistics, Volume 1*, M. Armstrong (ed.), Kluwer Academic Publishers, Boston, pp. 295–308.

Starks, T.H. and Fang, J.H. (1982) The effect of drift on the experimental semivariogram. *Mathematical Geology*, **14**, 309–20.

Thompson, S.K. (1990) Adaptive cluster sampling. *Journal of the American Statistical Association*, **85**, 1050–9.

Thompson, S.K., Ramsey, F.L., and Seber, G.A.F. (1992) An adaptive procedure for sampling animal populations. *Biometrics*, **48**, 1195–9.

Biographical sketches

Frank Curriero is an assistant scientist in the Department of Biostatistics at Johns Hopkins University. Dr Curriero received his Ph.D. in Statistics from Kansas State University in 1996 and spent two years as a postdoctoral researcher at the West Virginia Geological and Economic Survey. His current research interests include methods and applications of spatial statistics to public health and ecology.

Michael Hohn is Senior Research Geologist with the West Virginia Geological and Economic Survey, where he applies quantitative methods to researching the occurrence and quantity of fuel and nonfuel minerals, oil and natural gas. His interest in spatial statistics has led to work with geographers and entomologists in cross-disciplinary studies of forest pests, deer populations, and human demographics. Dr Hohn received his Ph.D. in Geology from Indiana University in 1976, spent two years as a postdoctoral researcher at the School of Chemistry, Bristol University, England, and has been at the Survey since 1978.

Andrew Liebhold has been a research entomologist with the USDA Forest Service North-Eastern Research Station, Morgantown, West Virginia, U.S.A. for 13 years. His research focuses on various aspects of the population ecology of forest insects, mainly emphasizing spatial aspects of population dynamics. As part of this research, Dr Liebhold has engaged various applications of spatial statistics to a variety of ecological data. He received a Ph.D. in entomology at the University of California, Berkeley in 1984 and spent four years as a postdoctoral at the University of Massachusetts.

Subhash Lele is Associate Professor in the Department of Mathematical Sciences at the University of Alberta, Canada. He was a member of a U.S. National Research Council panel on Global Climate Change and Public Health issues. He was recently awarded (jointly with two biologists) a Canada Foundation for Innovation grant to establish a Spatial Statistics, GIS and Ecology program. His current research interests are in Generalized Linear Mixed Models and Spatial Statistics with applications in public health and ecology.